

The following resources related to this article are available online at www.sciencemag.org (this information is current as of September 24, 2009):

Updated information and services, including high-resolution figures, can be found in the online version of this article at:

<http://www.sciencemag.org/cgi/content/full/289/5480/756>

This article **cites 15 articles**, 5 of which can be accessed for free:

<http://www.sciencemag.org/cgi/content/full/289/5480/756#otherarticles>

This article has been **cited by** 288 article(s) on the ISI Web of Science.

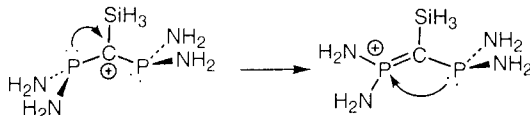
This article has been **cited by** 64 articles hosted by HighWire Press; see:

<http://www.sciencemag.org/cgi/content/full/289/5480/756#otherarticles>

Information about obtaining **reprints** of this article or about obtaining **permission to reproduce this article** in whole or in part can be found at:

<http://www.sciencemag.org/about/permissions.dtl>

Fig. 7. Cascade stabilization in diphosphino-substituted carbocations.



corresponding *P*-methyl phosphorus ylide **3** in near-quantitative yield (an ylide is a compound in which a positively charged atom from group 15 or 16 is connected to a carbon atom carrying a negative charge) (Fig. 2). Further investigation of **2'** through analysis of the Laplacian of the electron density (20) and the electron localization function (21) reveals a strong "banana" P–P bond with large *p* character (the bond ellipticity is 0.45) in the plane of the ring and partial double-bond character (Wiberg bond indices = 1.2) for the P–C bonds (Fig. 5).

The calculations found that the open planar form (C_{2v} symmetry) of type **1'a**, analogous to that of amidinium salts, is not a minimum on the potential energy surface. This illustrates the striking difference between phosphorus and nitrogen chemistry (Fig. 6). However, pyramidalization at one of the phosphorus atoms leads to **1'b**, which is not only an energy minimum, but is also lower in energy by 24 kJ/mol than the cyclic form **2'**. The experimental observation of **2** can be explained by the presence of bulky diisopropylamino groups because the steric demand in the linear form is larger than in the cyclic system.

Derivative **2** can be considered as resulting from a "cascade stabilization" of the electron-deficient carbocation center. As in the case of monophosphinocarbenium ions such as **A**, the first phosphorus atom gives electrons to the carbocationic center and becomes positively charged and, therefore, highly electrophilic (22). The second phosphorus atom then acts as a Lewis base toward the first (Fig. 7).

This type of transformation of a cationic center into an anionic center is unlikely to be unique and should be of important synthetic utility. For example, preliminary calculations predict that the corresponding diphosphonitrenium ions should exist in the cyclic form, with a negatively charged nitrogen atom. The synthesis of **2**, combined with the recent preparation of a tricyclic tetraphosphabenzene valence isomer (23) (calculated in the carbon series to be 933 kJ/mol less stable than benzene), also suggests that the unique electronic properties of heavier main-group elements will allow for the preparation of many new structural moieties that are difficult or impossible to access in the corresponding carbon and nitrogen series.

References and Notes

- G. A. Olah, *J. Am. Chem. Soc.* **94**, 808 (1972).
- _____, *Angew. Chem. Int. Ed. Engl.* **34**, 1393 (1995).
- _____, and P. von R. Schleyer, Eds., *Carbocation Ions* (Wiley, New York, 1976).
- R. A. Volkmann, in *Comprehensive Organic Synthesis*, B. M. Trost, Ed. (Pergamon, Oxford, 1991), vol. 1, pp. 355–396.

- P. Vogel, Ed., *Carbocation Chemistry* (Elsevier, Amsterdam, 1985).
- M. Saunders and H. A. Jiménez-Vázquez, *Chem. Rev.* **91**, 375 (1991).
- G. A. Olah, *Angew. Chem. Int. Ed. Engl.* **32**, 767 (1993).
- H. Grützmacher and C. M. Marchand, *Coord. Chem. Rev.* **163**, 287 (1997).
- W. W. Schoeller and U. Tubbesing, *Inorg. Chem.* **37**, 3183 (1998).
- M. J. Frisch et al., *Gaussian 98 (Revision A.1)* (Gaussian, Pittsburgh, PA, 1998).
- A. Göller, H. Heydt, T. Clark, *J. Org. Chem.* **61**, 5840 (1996).
- V. I. Minkin, M. N. Glukhovtsev, B. Ya. Simkin, Eds., *Aromaticity and Antiaromaticity: Electronic and Structural Aspects* (Wiley, New York, 1994).
- A. Igau, A. Baceiredo, G. Trinquier, G. Bertrand, *Angew. Chem. Int. Ed. Engl.* **28**, 621 (1989).
- A. Igau, A. Baceiredo, H. Grützmacher, H. Pritzkow, G. Bertrand, *J. Am. Chem. Soc.* **111**, 6853 (1989).
- O. Guerret and G. Bertrand, *Acc. Chem. Res.* **30**, 486 (1997).
- A. H. Cowley, M. C. Cushner, J. S. Szobota, *J. Am. Chem. Soc.* **100**, 7784 (1974).
- F. Mathey, *Chem. Rev.* **90**, 997 (1990).
- E. Breitmaier and W. Voelter, Eds., *Carbon-13 NMR Spectroscopy* (VCH, Weinheim, Germany, 1990).
- Crystal data for **2** is as follows. Cell constants and an orientation matrix for data collection correspond to the monoclinic space group $P2_1/c$, with the following cell parameters: $a = 15.031(2)$ Å, $b = 10.218(1)$ Å, $c = 24.906(3)$ Å, $\beta = 100.99(1)^\circ$, and V (cell volume) = 3755.1(8) Å³. There is one molecule, $C_{29}H_{65}F_3N_4O_3P_2SSi$, per asymmetric unit (number of formula units per cell = 4), giving a formula weight of

696.94 and a calculated density D_c of 1.233 Mg m⁻³. The data of the structure were collected on a STOE Imaging Plate Diffraction System diffractometer at a temperature of 173(2) K with graphite-monochromated Mo K α radiation (wavelength = 0.71073 Å) by using φ scans. We solved the structure by direct methods, using SHELXS-97 [G. M. Sheldrick, *Acta Crystallogr.* **A46**, 467 (1990)]. The linear absorption coefficient, μ , for Mo K α radiation is 0.252 mm⁻¹. The structure was refined with all data on F^2 with a weighting scheme of $w^{-1} = \sigma^2(F_o^2) + (g_1 \cdot P)^2 + (g_2 \cdot P)$ with $P = (F_o^2 + 2F_c^2)/3$ using SHELXL-97 [G. M. Sheldrick, *Program for Crystal Structure Refinement* (Universität Göttingen, Göttingen, 1997)] [g is the weighting factor ($g_1 = 0.069100$ and $g_2 = 3.406500$), and F_o and F_c are the observed and calculated structure factors, respectively]. All nonhydrogen atoms were treated anisotropically. The hydrogen atoms were located by difference Fourier maps and refined with a riding model. The final cycle of full-matrix least squares refinement was based on 21,874 measured (5180 unique) reflections and 407 variable parameters and converged with the unweighted agreement factor equal to $R1$ [$I > 2\sigma(I) = 0.0484$ (I is the observed reflection intensity)] and the weighted factor $wR2 = 0.1328$ for all data. Crystallographic details are available at www.sciencemag.org/feature/data/1051650.shl.

- R. F. W. Bader, Ed., *Atoms in Molecules* (Clarendon, Oxford, 1994).
- A. D. Becke and K. E. Edgecombe, *J. Chem. Phys.* **92**, 5397 (1990).
- Because of the opposite electronegativity difference for nitrogen-carbon and phosphorus-carbon atoms, calculations predict that the R_2N and R_2P fragments of iminium ($R_2N=C<$)⁺ and methylenephosphonium ($R_2P=C<$)⁺ ions bear a negative and positive charge, respectively.
- Y. Canac et al., *Science* **279**, 2080 (1998).
- We are grateful to the French Embassy in Japan for a grant to T.K. and to the Centre National de la Recherche Scientifique and Deutsche Forschungsgemeinschaft for financial support of this work.

26 April 2000; accepted 23 June 2000

Atmospheric Influence of Earth's Earliest Sulfur Cycle

James Farquhar,* Huiming Bao, Mark Thiemens

Mass-independent isotopic signatures for $\delta^{33}S$, $\delta^{34}S$, and $\delta^{36}S$ from sulfide and sulfate in Precambrian rocks indicate that a change occurred in the sulfur cycle between 2090 and 2450 million years ago (Ma). Before 2450 Ma, the cycle was influenced by gas-phase atmospheric reactions. These atmospheric reactions also played a role in determining the oxidation state of sulfur, implying that atmospheric oxygen partial pressures were low and that the roles of oxidative weathering and of microbial oxidation and reduction of sulfur were minimal. Atmospheric fractionation processes should be considered in the use of sulfur isotopes to study the onset and consequences of microbial fractionation processes in Earth's early history.

The present-day sulfur cycle is strongly influenced by anthropogenic emissions, biological processes, and oxidative weathering of continental sulfides (1–3). It has been debated whether the sulfur cycle early in Earth's

history was significantly different from the preanthropogenic sulfur cycle (4–9). Here we report sulfur multiple-isotope measurements (of $\delta^{33}S$, $\delta^{34}S$, and $\delta^{36}S$) of sulfide and sulfate minerals from Precambrian sedimentary and metasedimentary rocks and use them to document that a profound change occurred in the sulfur cycle between 2090 and 2450 Ma.

Thermodynamic, kinetic, and biological processes produce isotopic fractionations that depend on the relative mass differences be-

Department of Chemistry and Biochemistry, University of California, San Diego, La Jolla, CA 92093, USA. E-mail: jfarquha@ucsd.edu (J.F.); hbao@ucsd.edu (H.B.); and MHT@chem.ucsd.edu (M.T.)

*To whom correspondence should be addressed.

REPORTS

tween different isotopes of sulfur and oxygen. As a result, observed isotope variation can be related by $\delta^{33}\text{S} = 0.515 \times \delta^{34}\text{S}$, $\delta^{36}\text{S} = 1.90 \times \delta^{34}\text{S}$, and $\delta^{17}\text{O} = 0.52 \times \delta^{18}\text{O}$ (10). The quantities $\Delta^{33}\text{S}$, $\Delta^{36}\text{S}$, and $\Delta^{17}\text{O}$ (11) reflect the deviation of measured isotope compositions ($\delta^{33}\text{S}$, $\delta^{34}\text{S}$, and $\delta^{36}\text{S}$, or $\delta^{17}\text{O}$ and $\delta^{18}\text{O}$) from mass fractionation arrays with origins at $\delta^{33}\text{S}_{\text{CDT}} = 0$, $\delta^{34}\text{S}_{\text{CDT}} = 0$, and $\delta^{36}\text{S}_{\text{CDT}} = 0$ for sulfur, and at $\delta^{17}\text{O}_{\text{SMOW}} = 0$ and $\delta^{18}\text{O}_{\text{SMOW}} = 0$ for oxygen (CDT, Canyon Diablo Troilite; SMOW, standard mean ocean water).

In addition, several isotopic fractionation processes are also known to produce mass-independent compositions ($\Delta^{33}\text{S} \neq 0$, $\Delta^{36}\text{S} \neq 0$, or $\Delta^{17}\text{O} \neq 0$) (12–14). These include fractionations that result from hyperfine interactions in solid and liquid phases and an increasing number of gas-phase reactions (13). The hyperfine effect derives from spin-orbit coupling in isotopes with odd-mass nuclei and is therefore limited to isotopomers that contain these nuclei (such as ^{33}S and ^{17}O). Gas-phase mass-independent fractionations have been documented for a number of sulfur phases in laboratory experiments (SO_2 , H_2S , CS_2 , and S_2F_{10}) (12, 15, 16), but the physical chemical origin of the effect is still uncertain. The role of gas-phase mass-independent chemistry in determining the oxygen isotopic compositions of many atmospheric species is unequivocal (13), and these types of reactions may also play an important role in determining the sulfur isotope compositions of atmospheric species (15).

To examine sulfur isotope variability in early Earth, we extracted sulfur from sulfide and sulfate minerals in a variety of Precambrian samples. Sulfur isotopic analyses fall into two groups defined on the basis of $\Delta^{33}\text{S}$ values and geological age (Fig. 1; also see Web table 1 at www.sciencemag.org/feature/data/1052160.shl). Samples younger than 2090 Ma display a range of $\Delta^{33}\text{S}$ values from -0.11 per mil (‰) to 0.02 ‰ and are consid-

ered to be consistent with fractionation by mass-dependent processes. Sulfide and sulfate samples older than 2090 Ma but younger than 2450 Ma exhibit a range of $\Delta^{33}\text{S}$ varying between 0.02 and 0.34‰, and samples older than 2450 Ma exhibit a much larger range of $\Delta^{33}\text{S}$, varying between -1.29 and 2.04‰. This variation is consistent with large mass-independent compositions. The relation between $\Delta^{33}\text{S}$ and $\Delta^{36}\text{S}$ (Fig. 2) and between $\delta^{36}\text{S}$ and $\delta^{34}\text{S}$ for samples older than 3000 Ma (Fig. 3) rules out the possibility that hyperfine interactions account for the observations. The most likely explanation of observed $\Delta^{33}\text{S}$ and $\Delta^{36}\text{S}$ values for early Proterozoic and Archean sulfide and sulfate is, therefore, the presence of one or more gas-phase, mass-independent chemical reactions in the sulfur cycle.

Photochemical reactions are thought to be important in the early Proterozoic and Archean atmosphere and may be relevant to the sulfur cycle before 2090 Ma. Photochemical reactions have been suggested as the source of nonzero $\Delta^{33}\text{S}$ values in martian samples (martian meteorites) (15). Our data indicate that a profound change occurred in the sulfur cycle between 2090 and 2450 Ma. This change might represent the onset of a process capable of homogenizing mass-independently fractionated sulfur reservoirs or the suppression of one or more atmospheric reactions that had occurred before this interval.

Two basic models have been suggested for Earth's early sulfur cycle. The first is that the Archean sulfur cycle did not differ significantly from the preanthropogenic sulfur cycle (7–9) and that the dominant source of oceanic sulfate was oxidative weathering of continental sulfides and weathering of continental sulfates. The second is that oxidative weathering did not play a significant role in the Archean sulfur cycle and that the principal source of oceanic sulfate was photochemical oxidation of volcanogenic sulfur species in the Archean atmosphere (6). Our mass-

independent sulfur isotope data strongly support a pre-2090-Ma sulfur cycle that was influenced by atmospheric chemical reactions. All of our data for samples of barite and of barite plus chert that are older than 2090 Ma have negative $\Delta^{33}\text{S}$ values. One analysis of Archean barite from the Sargur Group of Karnataka, India (17), also yielded a negative $\Delta^{33}\text{S}$ value. Most of our data for samples of pelitic and psammitic rocks older than 2090 Ma have positive $\Delta^{33}\text{S}$ values. These observations are consistent with the existence of two reservoirs: a water-soluble (oceanic?) sulfate reservoir with negative $\Delta^{33}\text{S}$ values and an insoluble reservoir of reduced sulfur with positive $\Delta^{33}\text{S}$ values. Oxidative weathering would have mixed these reservoirs by transferring sulfur from reduced to oxidized reservoirs, producing sulfate with a positive (or juvenile) $\Delta^{33}\text{S}$ signature that would dilute (or even eliminate) the negative $\Delta^{33}\text{S}$ signature of its global oceanic counterpart. We infer that the transition to a sulfur cycle more like the modern preanthropogenic sulfur cycle occurred after 2090 Ma, when higher levels of atmospheric oxygen overwhelmed the atmospheric sources of oceanic sulfate through oxidative and microbial weathering of continental sulfides. Further insight into the nature of this transition will be obtained once the atmospheric reaction (or reactions) responsible for producing the effect are identified.

It is also possible that the atmospheric chemistry responsible for producing the observed mass-independent sulfur isotopic compositions before 2090 Ma may have stopped operating as a result of a change in atmospheric composition or actinic flux. Some have suggested that changes in the solar spectrum [ul-

Fig. 1. Plot of $\Delta^{33}\text{S}$ values versus sample age. Variable $\Delta^{33}\text{S}$ values for samples with geological ages greater than the transition interval at 2090 to 2450 Ma are interpreted as an indication of atmospheric influence of the sulfur cycle. Homogeneous $\Delta^{33}\text{S}$ values for samples with geological ages less than 2090 Ma are interpreted as an indication of a sulfur cycle dominated by oxidative weathering of continental sulfide and sulfate. The dark gray band at $\Delta^{33}\text{S} \sim 0$ represents the mean and 1 SD of data collected to date from younger sulfide and sulfate from 73 samples that include mantle xenoliths, marine barite, desert gypsum, evaporite, massive pyrite, channel deposits, ash deposits, and building surface deposits. Age data for these samples are compiled in (30).

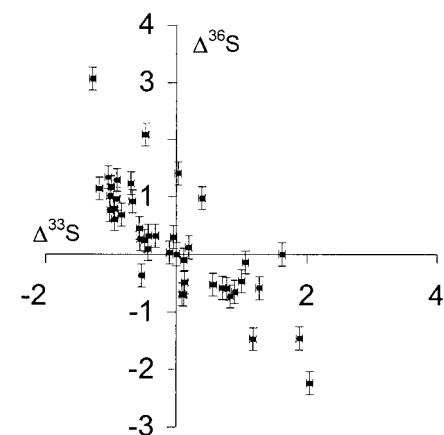
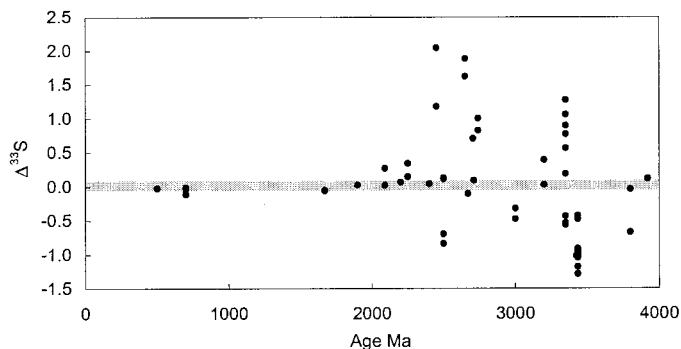


Fig. 2. Plot of $\Delta^{33}\text{S}$ versus $\Delta^{36}\text{S}$ for samples older than 2090 Ma. The correlation between $\Delta^{33}\text{S}$ and $\Delta^{36}\text{S}$ is interpreted as evidence of mass-independent isotopic fractionations originating in gas-phase reactions rather than from hyperfine interactions, which would produce $\Delta^{33}\text{S}$ but not $\Delta^{36}\text{S}$. Mass-dependent processes plot at the origin of this plot. Error bars represent 1σ analytical uncertainties of 0.05 and 0.3‰ for $\Delta^{33}\text{S}$ and $\Delta^{36}\text{S}$, respectively.

traviolet (UV) and visible wavelengths] resulting from main sequence brightening (18) could have affected atmospheric chemistry in Earth's earliest atmosphere (19, 20). Although this change may account for our observations, changes in the abundance of absorbing species in the upper atmosphere exert a much stronger influence on lower atmospheric UV and on photochemistry (21). Higher surface UV resulting from a reduced ozone column depth in an atmosphere with low oxygen concentrations (22–24) may have played a role in determining atmospheric sulfur chemistry and in generating isotopically distinct sulfur reservoirs. Photolysis of SO₂, for instance, results in production of SO₃ (25) that converts to H₂SO₄ upon contact

with water. This photochemical oxidation sequence has been shown to produce mass-independently fractionated sulfur (15). Whereas oxygen isotopic signatures of present-day products of atmospheric oxidation of reduced sulfur-bearing gases have been shown to possess mass-independent oxygen isotopic compositions that are thought to be the result of oxidation by isotopically anomalous ozone and hydrogen peroxide (26, 27), our oxygen isotope data for sulfate from barites from 3300 to 3400 Ma are mass-dependent ($\Delta^{17}\text{O} = 0.01 \pm 0.06\text{‰}$). The lack of a similar mass-independent signature in our Archean barites may be a further indication that the sulfur oxidation pathways were different from that of the current atmosphere, possibly reflecting the exchange of sulfite (a product of SO₂ photooxidation) with water during the formation of sulfate. If this is the case, the buildup of atmospheric oxygen may have helped shut down the atmospheric chemical reactions that were responsible for generating isotopically anomalous sulfur-bearing reservoirs. An alternative explanation of the oxygen isotope data is that the original atmospheric oxygen isotopic signature has been lost because of exchange processes that occurred after sulfate formation.

If $\delta^{33}\text{S}$ fractionations reflect atmospheric fractionation processes, it is also possible that the same applies to $\delta^{34}\text{S}$ fractionations. Some workers have divided the sulfur isotope record into a period before 2750 Ma, when the range of $\delta^{34}\text{S}$ was less than about 10‰, and a period after 2750 Ma, when the range of $\delta^{34}\text{S}$ was greater than 10‰ (5, 28). These workers suggest that the change in magnitude for the range of observed $\delta^{34}\text{S}$ fractionations at 2750 Ma is evidence of the onset of microbial sulfate reduction. Other workers have suggested that the smaller range of $\delta^{34}\text{S}$ before 2750 Ma also results from microbial sulfate reduction but at higher temperature conditions, possibly at lower oceanic sulfate concentrations or in closed systems (7–9). On three isotope plots (Fig. 3), our data do not follow the mass-dependent arrays that would be formed by microbial sulfate reduction (for example, $\delta^{33}\text{S} \sim 0.515 \times \delta^{34}\text{S}$ and $\delta^{36}\text{S} = 1.90 \times \delta^{34}\text{S}$), and they allow that the $\delta^{34}\text{S}$ record for samples older than 2750 Ma may be entirely atmospheric in origin. Although our data do not rule out the possibility of microbial sulfate reduction, they imply that $\delta^{34}\text{S}$ values cannot be used alone to argue for the operation of (or examine the consequences of) metabolic processes that fractionated sulfur isotopes before 2750 Ma.

Similar sulfur isotope measurements can be used to resolve atmospheric inputs and to gain new insights into biogeochemical element cycles. The recent observation of mass-independently fractionated sulfur in this study and in martian meteorites (15) and of mass-independently fractionated oxygen in terrestrial and martian sulfates (27, 29) opens

up possibilities for identifying additional components of the sulfur cycle on Earth and on other bodies in the solar system.

References and Notes

1. A. Paytan, M. Kastner, D. Campbell, M. H. Thiemens, *Science* **282**, 1459 (1998).
2. R. A. Berner and R. Raiswell, *Geochim. Cosmochim. Acta* **47**, 855 (1983).
3. P. Brimblecombe, C. Hammer, H. Rodhe, A. Ryaboshapko, C. F. Boutron, in *Evolution of the Global Biogeochemical Sulphur Cycle*, P. Brimblecombe and A. Y. Lein, Eds. (Wiley, New York, 1989), pp. 77–121.
4. E. M. Cameron, *Nature* **296**, 145 (1982).
5. I. B. Lambert and T. H. Donnelly, in *Early Organic Evolution: Implications for Mineral and Energy Resources*, M. G. Schidlowski, S. Golubic, M. M. Kimberley, D. M. McKirdy, P. A. Trudinger, Eds. (Springer-Verlag, New York, 1992), pp. 408–415.
6. J. C. G. Walker and P. Brimblecombe, *Precambrian Res.* **28**, 205 (1985).
7. H. Ohmoto, T. Kakegawa, D. R. Lowe, *Science* **262**, 555 (1993).
8. H. Ohmoto and R. P. Felder, *Nature* **328**, 244 (1987).
9. T. Kakegawa and H. Ohmoto, *Precambrian Res.* **96**, 209 (1999).
10. J. R. Hulston and H. G. Thode, *J. Geophys. Res.* **70**, 3475 (1965).
11. Those quantities are as follows: $\Delta^{33}\text{S} = 1000 \times [(1 + \delta^{33}\text{S}/1000) - (1 + \delta^{34}\text{S}/1000)^{0.518} - 1]$, $\Delta^{36}\text{S} = 1000 \times [(1 + \delta^{36}\text{S}/1000) - (1 + \delta^{34}\text{S}/1000)^{1.91} - 1]$, and $\Delta^{17}\text{O} = 1000 \times [(1 + \delta^{17}\text{O}/1000) - (1 + \delta^{18}\text{O}/1000)^{0.52} - 1]$. Uncertainties for $\Delta^{33}\text{S}$, $\Delta^{36}\text{S}$, and $\Delta^{17}\text{O}$ are better than ± 0.05 , 0.3, and 0.05‰, respectively.
12. P. Zmolek, X. P. Xu, T. Jackson, M. H. Thiemens, W. C. Troglor, *J. Phys. Chem.* **103**, 2477 (1999).
13. M. H. Thiemens, *Science* **283**, 341 (1999).
14. R. E. J. Weston, *Chem. Rev.* **99**, 2115 (1999).
15. J. Farquhar, J. Savarino, M. H. Thiemens, T. L. Jackson, *Nature* **404**, 50 (2000).
16. S. K. Bains-Sahota and M. H. Thiemens, *J. Chem. Phys.* **90**, 6099 (1989).
17. T. C. Hoering, *J. Geol. Soc. India* **34**, 461 (1989).
18. K. J. Zahnle and J. C. G. Walker, *Rev. Geophys. Space Phys.* **20**, 280 (1982).
19. V. M. Canuto, J. S. Levine, T. R. Augustsson, C. L. Imhoff, M. S. Giampapa, *Nature* **305**, 281 (1983).
20. C. Sagan and C. Chyba, *Science* **276**, 1217 (1997).
21. J. F. Kasting, H. D. Holland, L. R. Kump, in *The Proterozoic Biosphere: A Multidisciplinary Study*, J. W. Schopf and C. Klein, Eds. (Cambridge Univ. Press, New York, 1992), pp. 159–163.
22. J. F. Kasting, H. D. Holland, J. P. Pinto, *J. Geophys. Res.* **90**, 10497 (1985).
23. J. F. Kasting, *Precambrian Res.* **34**, 205 (1987).
24. _____, *Origins Life Evol. Biosph.* **20**, 199 (1990).
25. H. Okabe, *Photochemistry of Small Molecules* (Wiley, New York, 1978).
26. C. W. Lee, J. Savarino, M. H. Thiemens, *Am. Geophys. Union* **79**, F91 (1998).
27. H. Bao et al., *Nature*, in press.
28. A. M. Goodwin, J. Monster, H. G. Thode, *Econ. Geol.* **71**, 870 (1976).
29. J. Farquhar and M. H. Thiemens, *J. Geophys. Res.* **105**, 11991 (2000).
30. T. B. Moore and J. W. Schopf, in *The Proterozoic Biosphere: A Multidisciplinary Study*, J. W. Schopf and C. Klein, Eds. (Cambridge Univ. Press, New York, 1992), pp. 605–694.
31. D. York, *Earth Planet. Sci. Lett.* **5**, 320 (1969).
32. Supported by grants from NSF, NASA, and CalSpace. Samples used in this study were supplied and/or collected by J. W. Schopf, B. Runnegar, D. Lowe, H. Baadsgaard, and S. J. Mojzsis. The interpretations herein are our responsibility, but they have benefited from interesting conversations and questions from R. N. Clayton, K. Boering, T. Chacko, D. DePaolo, H. D. Holland, M. Humayun, J. Kasting, A. Knoll, S. J. Mojzsis, A. Payton, G. Retallack, and K. K. Turekian. We thank D. Canfield and J. Kasting for providing copies of in press and unpublished materials.

12 May 2000; accepted 9 June 2000

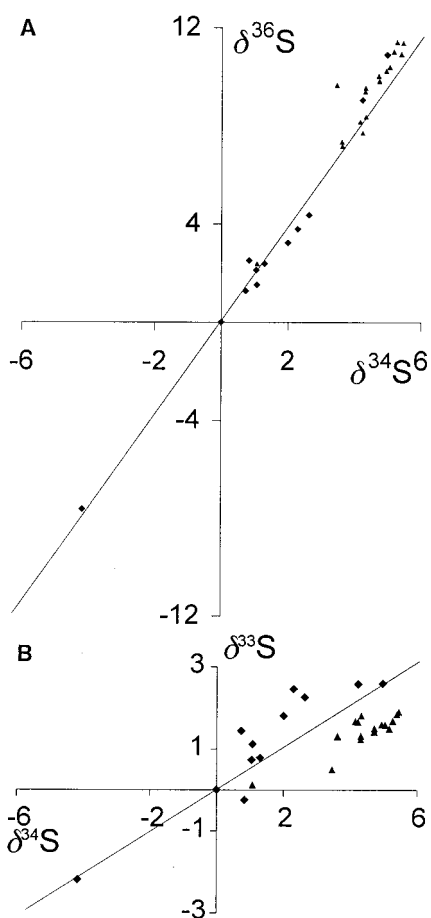


Fig. 3. Three isotope plots of (A) $\delta^{36}\text{S}$ versus $\delta^{34}\text{S}$ and (B) $\delta^{33}\text{S}$ versus $\delta^{34}\text{S}$ for samples older than 3000 Ma. The array formed on (A) follows the relation $\delta^{36}\text{S} = 2.17 (\pm 0.1) \times \delta^{34}\text{S}$ [calculated using York (37)] rather than the mass-dependent relation $\delta^{36}\text{S} = 1.90 (\pm 0.01) \times \delta^{34}\text{S}$ (10). The data in (B) do not follow the tightly constrained mass-dependent relation $\delta^{33}\text{S} = 0.515 (\pm 0.005) \times \delta^{34}\text{S}$ (10) but scatter on the diagram. Barite and chert-plus-barite samples are plotted as triangles. All other samples are plotted as diamonds. These arrays are inconsistent with biological fractionation processes and are consistent with a sulfur cycle that is strongly influenced by atmospheric chemical reactions and atmospheric oxidation reactions.